ON THE WINTER CIRCULATION OF THE NORTHERN SOUTH CHINA SEA AND ITS RELATION TO THE LARGE SCALE OCEANIC CURRENT*

PART I: NONWIND-DRIVEN CIRCULATION OF THE NORTHERN SOUTH CHINA SEA AND NUMERICAL EXPERIMENTS

Ma Hong(马 虹)

(*Institute of Oceanology, Academia Sinica, Qingdao*)

Received April 2, 1986

Abstract

The nonwind-driven mechanism of the winter circulation in the northern South China Sea is discussed.

Linked by the Bashi Strait to the Pacific Ocean, the northern South Cnina Sea is treated as a part of the Pacific western boundary where the circulation variation (except the very thin surface layer) is closely related to that of the ocean interior and the effect of local wind might be neglected (at least for some seasons).

Based on the assumption that the thick and strong westward current which flows in through the Bashi Strait can effectively prevent water exchange between the northern and southern South China Seas, the model sea only includes the northern part. Barotropic numerical experiments show that part of this westward current is deflected by the continental slope and forms the slope area NE current—the South China Sea Warm Current. Besides, the topographical flow fed by the extension of the western boundary current and the anticyclonic eddy born near the eastern boundary are also fundamental components of the South China Sea Warm Current. The reflection of the incident Rossby waves by the continental slope is found to be of significance in the intensification of the South China Sea Warm Current.

I. INTRODUCTION

The South China Sea is one of the biggest marginal seas in the western Pacific, and is a typical monsoon area.

Traditionally its surface current pattern and circulation in the northern part are thought to be in accord with the local wind direction, which is northeastward in summer and southwestward in winter. This opinion had been widely accepted until Guan Bingxian (1978)** proposed that in winter, along the continental slope off Guangdong Province, there was a narrow band of strong northeastward current flowing against the wind, and that this current was the strongest in this season, with volume transport of about one third of that of the Kuroshio. He named it the South China Sea Warm Current (Fig. 1). He made this discovery by analysing CSK data.

Four years later, the existence of the South China Sea Warm Current was confirmed by oceanographic observation, and the coexistence of the southwestward current on the right side of the South China Sea Warm Current was also revealed (Fig. 2). The study by Gue Zhungxen, Yang Tianhong, and Chou Dezhung (1984) showed that this southwestward current was a branch of the Kuroshio and was not driven by the local wind. The forming mechanism of the South China Sea Warm Current had not been discussed yet then.

---

*Contribution No. 1362 from Institute of Oceanology, Academia Sinica, Qingdao.

**Evidences of counter-wind current were observed in the shallow water region off Shantou and east of Hainan Island at the end of the fifties (Guan Bingxian and Chen Shangji, 1964. The Current Systems in the Seas Adjacent to China).

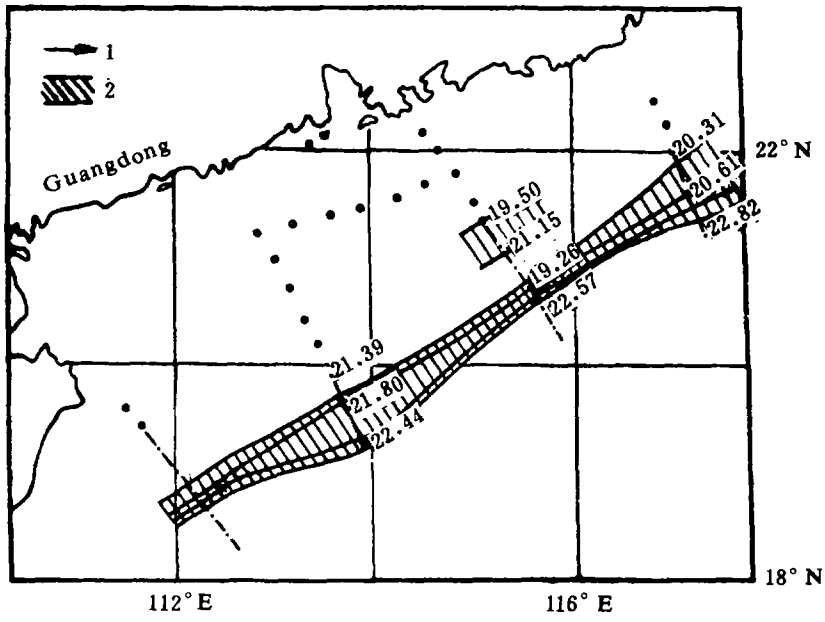

Fig. 1 The northern South China Sea 100 m depth temperature (°C) distribution, Jan. 6–14, 1968. (after ref. [1])
1. dyn. mm line 0 200 db
2. Area with temperature decreasing northward

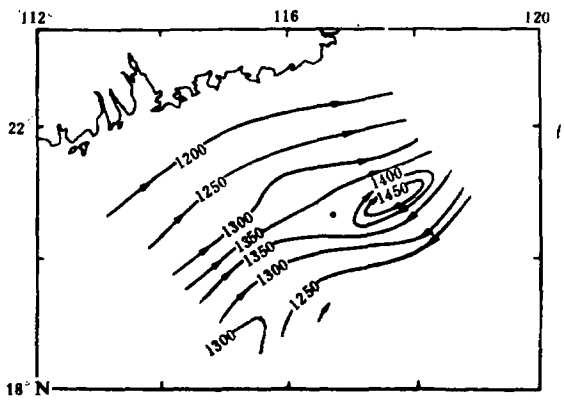

Fig. 2a Surface dynamic height distribution relative to 500 dyn. mm

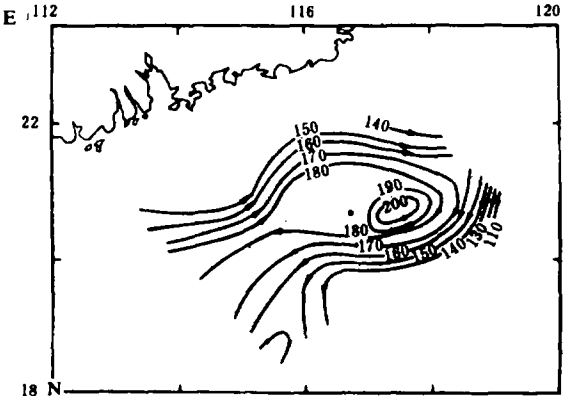

Fig. 2b Depth distribution (m) of $\sigma_t = 25.00$ (Fig. 2a, 2b are after ref. [3])

The Bashi Strait is the main passage for water exchange between the South China Sea and the western Pacific. Huang Qizhou (1983) studied the velocity and transport structure in the Bashi Strait in detail. His results show that across the meridional transection in the Bashi Strait the southern half is controlled by the westward transport and the northern half by the eastward transport (Fig. 3). The transport magnitudes are both about ten 10^6 m^3/s. The net westward transport peak is in winter and the valley in summer.[8,14]

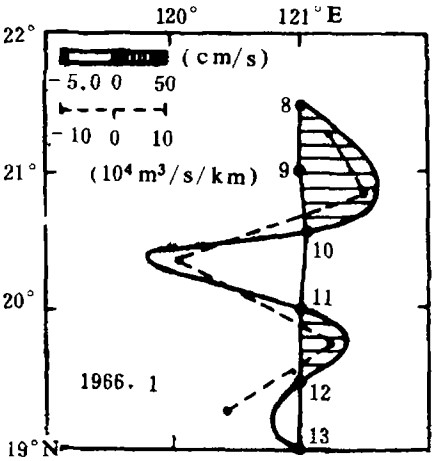

Fig. 3 Winter surface velocity and transport in the Bashi Strait (meridional section) (after ref. [5])

The research and observation results on the winter circulation pattern in the northern South China Sea can be summarized as follows:

1. In the deep water off Guangdong Province there is a northeastward current—the South China Sea Warm Current. It is relatively weak west of Dung Sha Island and strong east of it.

2. The southwestward current flows into the South China Sea through the Bashi Strait and can reach the western part of the South China Sea. Compared with the South China Sea Warm Current, its transport is somewhat higher but the spatial variation is much less obvious.

3. The strength of the South China Sea Warm Current and that of the westward transport through the Bashi Strait have similar seasonal variations.

II. THE NONWIND-DRIVEN MECHANISM OF THE NORTHERN CIRCULATION IN THE SOUTH CHINA SEA IN WINTER AND THE NUMERICAL EXPERIMENTS

1. Formation of the main idea

Though the South China Sea Warm Current can be observed throughout the year, it is most pronounced in winter during the northeast monsoon. This astonishing fact has stimulated researchers to re-examine the existing concept of the current forming mechanism in the South China Sea, because both the direction and the depth of this current can not be explained by the local wind field which has been considered as the major driving force of the surface circulation in the South China Sea.

The South China Sea Warm Current is like western boundary current in several aspects, such as narrow current width, high velocity, movement along the continental slope with eddies on both sides, etc. In addition, the South China Sea Warm Current, the westward transport through the Bashi Strait and the North Equatorial Current have the same tendency of seasonal strength variation. This phenomenon suggests that these currents have some relation with each other.

In the northern South China Sea the surface density distribution is very homogeneous in winter, with sigma t about 23.5 kgm^{-3} and delta st about 430 clt^{-1}. But in the southern part sigma t is below 22 kgm^{-3} and delta st is above 600 clt^{-1}. This means that there is a great difference between the northern and southern water masses in winter. From a study of the salinity distribution we can also find that there is a high salinity tongue extending from the Bashi Strait to Hainan Island in winter and that the northern isohalines stretch almost zonally*[6]. The difference in characteristics between the northern and southern water masses can be explained as follows: In

* Preliminary Data Report of CSK NOs 82, 92 Japanese Oceanographic Data Center.

winter, the strong southwestward current flowing in through the Bashi Strait runs from the eastern to the western South China Sea, and can reach a depth of 800 m. This 'flowing wall' effectively prevents water masses from exchanging meridionaly, so that the northern basin of the South China Sea has become a relatively isolated system in winter. As the bottom topography of the northwestern part of the South China Sea satisfies the inertial current existing condition $U\frac{\partial}{\partial y}\left(\frac{f}{h}\right) > 0$, when the southwestward current reaches the western boundary it may turn wholly or partly north to form the inertial boundary current.

Based upon the facts stated above, numerical experiments of the northern circulation have been designed in which the bottom topography of the northern South China Sea is simplified but still well represented and the Bashi Strait transport condition is taken as the sole external forcing source.

2. Basic assumptions

1) The model sea is composed of depth-variable one layer homogeneous water;

2) β plane and hydrostatic approximation are used;

3) Neglect the surface wind stress and the bottom friction and suppose the lateral friction is the major decay mechanism.

The South China Sea Warm Current and its right side southwestward current can reach a depth of 800 m, and the thickness influenced by the surface wind or the bottom friction is only about several tens of meters. Besides, the nature of these two currents precludes the possibility that they are wind-driven currents. In order to manifest the major physical process, the third assumption is adopted.

3. Governing equations

Under assumption (b) the equation of motion and the continuity equation can be written respectively as

$$\vec{V}_t + (\vec{V}\cdot\nabla)\vec{V} + f\vec{k}\Lambda\vec{V} = -g\nabla\eta + A_H\nabla^2\vec{V} \tag{1}$$

$$\frac{\partial\eta}{\partial t} + \nabla\cdot(h\vec{V}) = 0 \tag{2}$$

where $\vec{v}$ is the horizontal velocity vector; h is the thickness of the liquid layer; η is the surface elevation above that of no motion; A_H is the horizontal eddy viscosity coefficiet; f is the Coriolis parameter; and g is the constant of gravity acceleration.

Multiplying the vertical component of the curl operator with (1) gives the vorticity equation:

$$\frac{\partial Z}{\partial t} + \nabla\cdot((z+f)\vec{V}) = A_H\nabla^2 Z \tag{3}$$

Z is the vertical component of the curl: $\frac{\partial v}{\partial x} - \frac{\partial u}{\partial y}$.

Define the nondimensional variables as follows:

$$t = (\beta_0 L)^{-1}t' \qquad (x,y) = L(x',y')$$
$$\vec{V} = U\vec{V}' \qquad h = Hh'$$
$$f = \beta_0 L(F_0 + y') = \beta_0 LF' \qquad \eta = (\beta_0 L^2 U/g)\eta,$$

where $t', x', y', h', \eta', F', \vec{V}'$ are nondimensional variables and vector. U is defined as the averaged value in the vertical direction of the velocity of the South China Sea Warm Current, i.e. 10cms^{-1}; L is defined as the latitudinal scale of the northern South China Sea, i.e. 1,100 km; H is the depth of the surface circulation in the northern South China Sea, i.e. 1,000 m; $F_0 = 1.8$; $\beta_0 = 1.9 \times 10^{-13}$ s^{-1} cm^{-1}; $A_H = 10^8 cm^2\ s^{-1}$.

Substituting the nondimensional variables into equation (2) we have

$$(L^2/R^2)\frac{\partial \eta'}{\partial t'} + \nabla\cdot(h'\vec{V}') = 0 \tag{4}$$

where $R = \sqrt{gH}/\beta_0 L$ (which in the present situation is about 5,000 km). So the first term of (4) can be omitted, and equation (4) becomes

$$\nabla\cdot(h'\vec{V}') = 0 \tag{5}$$

From (5) we can introduce the volume transport stream function defined by $\vec{k}\Lambda\nabla\psi = h'\vec{V}'$ Then the nondimensionalized form of (3) can be written as

$$\frac{\partial Z}{\partial t} = \delta\nabla^2 Z - \nabla\cdot\left((\varepsilon Z + F)\vec{k}\Lambda\frac{\nabla\psi}{h}\right) \tag{6}$$

$$Z = \nabla\cdot\left(\frac{\nabla\psi}{h}\right) \tag{7}$$

where $\varepsilon = U/(\beta_0 L^2)$, $\delta = A_H/\beta_0 L^3$, and the mark of the nondimensional variables is omitted for simplicity.

4. Designing the model sea

We aim to demonstrate some physical mechanisms of the winter circulation in the northern South China Sea, so the geometric design should be as simple as possible. The rectangular basin between 111–121°E and 18.6–22°N is divided by 40 × 40 subrectangles, i.e. $\Delta x = 28.2$ km in the east-west direction and $\Delta y = 9.4$km in the north-south direction. Because the meridional flow state is more complex than the zonal flow state, so the meridional division is three times closer than the zonal division. The bottom topography is shallow in the northwest and deep in the southeast. The width of the continental slope is about 130 km (Fig.4).

5. Boundary conditions

The western boundary of the model sea is solid (viscous), the northern and southern boundaries are liquid (slippery). If we idealize the Bashi Strait transport condition as a sine function and neglect the opening of the Taiwan Strait because of its shallowness, then we can have the following boundary conditions:

$$\text{western boundary } (x = 0): \frac{\partial\psi}{\partial x} = 0, \quad \psi = 0$$

$$\text{eastern boundary } (x = 1): \frac{\partial\psi}{\partial x} = 0, \quad \psi = \sin(3\pi y)$$

$$\text{southern boundary } (y = 0): \frac{\partial^2\psi}{\partial y^2} = 0, \quad \psi = 0$$

$$\text{northern boundary } (y = 1/3): \frac{\partial^2\psi}{\partial y^2} = 0, \quad \psi = 0$$

6. Numerical method

C. Pearson (1965) proposed a method for solving two dimensional incompressible viscous flow problems, and our numerical scheme is the application of his method to the problem on a rotating planet with variable bottom topography. Analysis shows that the introduction of the nonlinearity and topography imposes a limitation on the time step Δt but our diference scheme is still superior to an explicit one because of the computation time saved.

Details of the numerical procedure were described in "The Nonwind-driven Circulation of the South China Sea and the Numerical Experiments"*.

* Ma Hong, 1985. M.S. thesis, Institute of Oceanology, Academia Sinica.

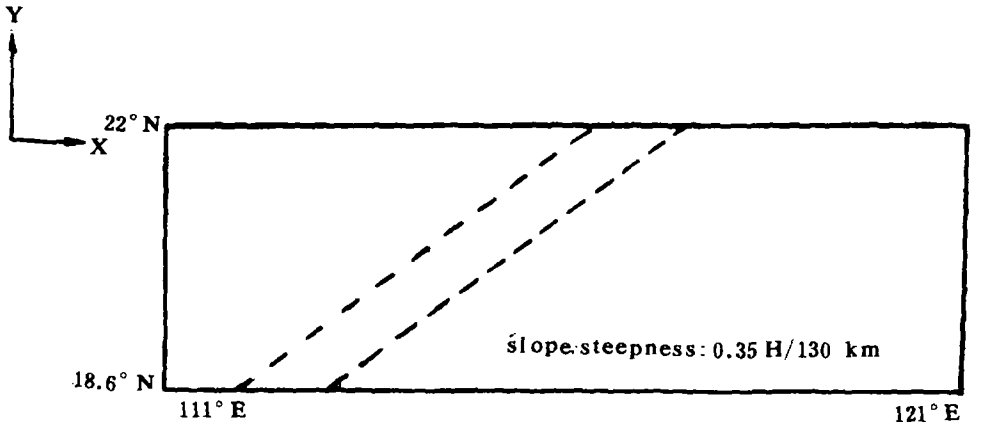

Fig. 4 Geometry of the model sea

7. Results of the numerical experiments

The time integration of the vorticity equation (6), which is combined with equation (7) and the boundary conditions, was carried out for 100 days from the initial state (in which the eastern boundary stream function values decreased evenly westward). The basic characteristics of the solution reached the quasi-steady state by the 45th day and so would not be distorted seriously by the limitation of the time integration (Figs. 5,6,7).

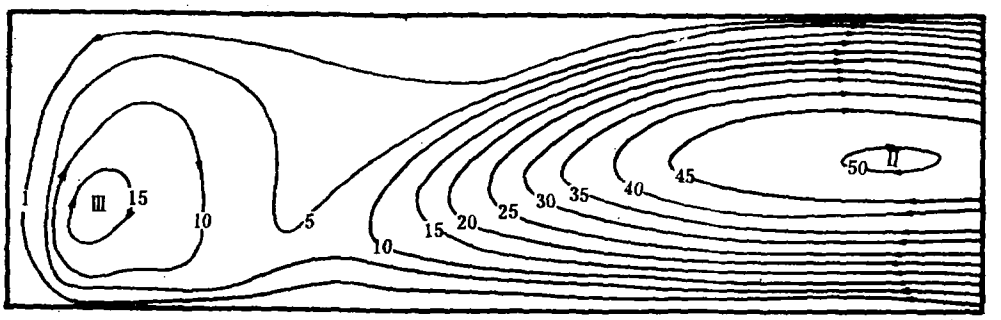

Fig. 5 Stream function contours ($50^{*}\psi$) time = 30th day

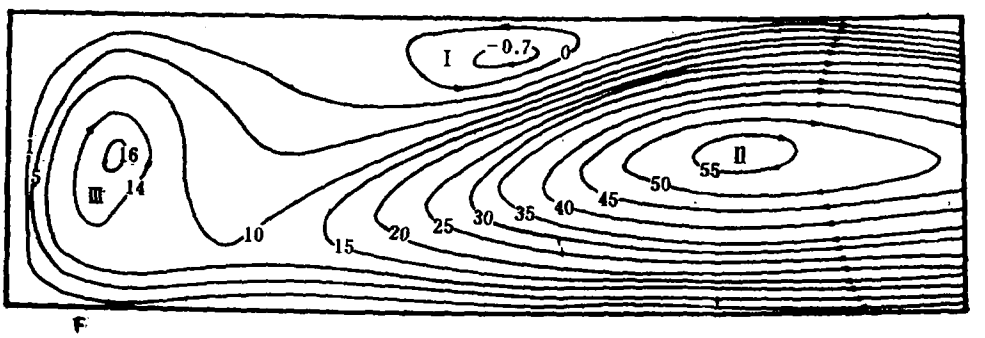

Fig. 6 Stream function contours ($50^{*}\psi$) time = 60th day

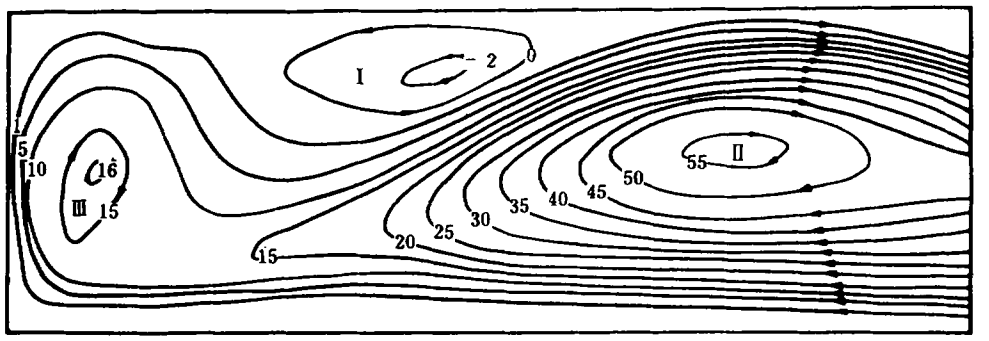

Fig. 7 Stream function contours (50*ψ) time = 90th day

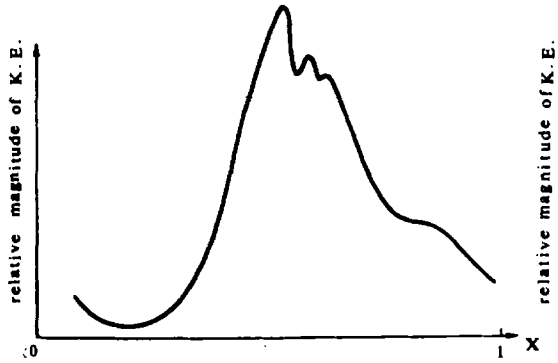

Fig. 8 Kinetic energy distribution along $\psi = 50*0.2$ in the NE flow

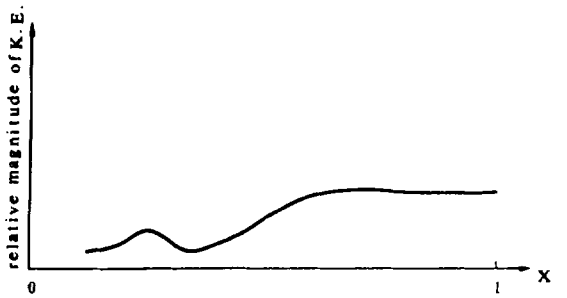

Fig. 9 Kinetic energy distribution along $\psi = 50*0.2$ in the SW flow

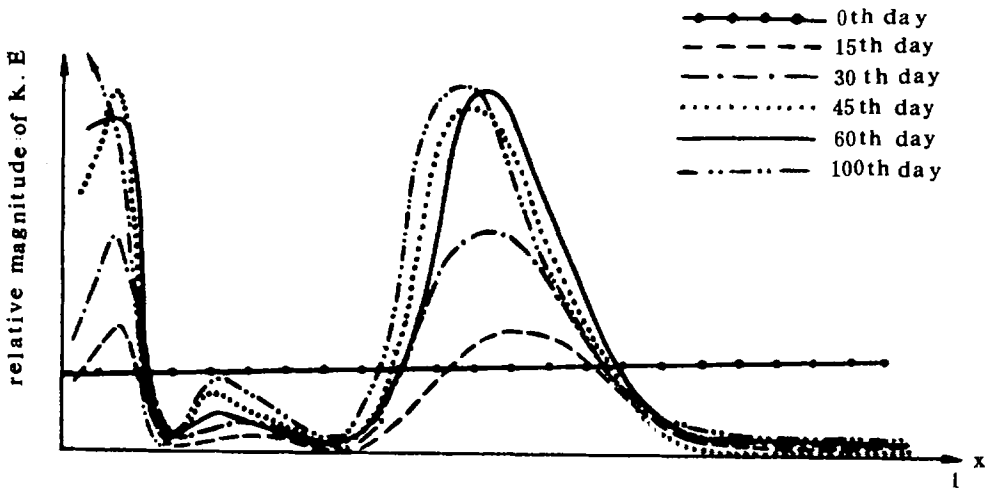

Fig. 10 K . $\mathcal{E}$ energy distribution along $y = 0.5$ at various times

The quasi-steady flow field had these major features: It had a strong NE current along the slope with the SW current on its right side, and three evident eddies. The space variation of the NE current was far greater than that of the SW current (Figs. 8,9). The path of the NE current meandered before extending into the slope area. There was a cyclonic eddy (I) in the valley. The anticyclonic eddy (II) between the NE current and the SW current was most energetic. Its center showed a strong tendency to move westward. Finally, there was an anticyclonic eddy (III) in the western shelf water.

From a comparison of the figures drawn from the observation data such as those shown in Fig. 2a, 2b, we found that the numerical experiments yielded quite satisfactory results.

8. Analysis of the numerical results

1) The northwestern meander

The stream function distribution in the western area shows great difference between the northern and the southern parts: there is a wavy meander in the northern part but none in the southern part. This phenomenon is due to the anisotropic response of the zonal flow to the perturbation of the bottom topography. If we assume the influence of the continental slope ruggedness can be represented by the fluctuation of the zonal flow with flat bottom, then from the vorticity equation (3), after simplification of the quasi-steady state and neglecting the friction and the boundary effects, we have:

$$u\frac{\partial}{\partial x}\left(\frac{\partial v}{\partial x}-\frac{\partial u}{\partial y}\right)+v\frac{\partial}{\partial y}\left(\frac{\partial v}{\partial x}-\frac{\partial u}{\partial y}\right)+\beta v=0 \tag{8}$$

Let

$$u=\bar{u}+u' \qquad v=v' \tag{9}$$

where $\bar{u}$ is the mean flow, u' and v' are the fluctuation components.

Substituting (9) into (8) and linearizing the equation, we get:

$$\bar{u}\frac{\partial^2 v'}{\partial x^2}+\beta v'=0 \tag{10}$$

Let

$$v'=Ae^{rx} \tag{11}$$

Substituting (11) into (10) gives

$$\bar{u}r^2+\beta=0 \tag{12}$$

Equation (12) provides a reasonable basis for explaining the previous phenomenon. If $\bar{u}>0$, i.e., in the northern part of the field, the solution of r is purely imaginary, v' has a solution in the form of the Rossby stationary wave, where the wave number $r=\sqrt{\beta/\bar{u}}$, and wave length $L=2\pi\sqrt{\bar{u}/\beta}$. $L=450$ km, when $\bar{u}=10$ cm/s and $\beta=1.9\times10^{-13}\mathrm{cm}^{-1}\mathrm{s}^{-1}$. Because of the damping effect of the friction, the topographical Rossby stationary wave should decay rapidly and the flow finally falls into the bottom of the topography – controlled area.

2) The intensification in the slope area and the eastern anticyclonic eddy

The NE current near the slope area is from three sources: the flow fed by the extension of the western boundary current, the directly deflected part of the westward flow because of the existence of the continental slope, and the eastern anticyclonic eddy. Like most of the western boundary currents, the NE current here also flows approximately along the slope isobath, exhibiting the nature of quasigeostrophic motion.

By the 20th day an anticyclonic eddy was formed near the eastern boundary. Its center moved

west at an average speed of 3.3 km/day. This value agrees with the theoretical results of the studies on the mesoscale eddy moving velocity reported by Warran (1967) and McWilliams (1979). The β effect is generally thought to be the mechanism responsible for the westward movement of the mesoscale eddies. The eastern anticyclonic eddy moved fast at first, then gradually slowed down and lingered about $x = 0.75$ (118.5°E) in the end (Fig. 11). The eddy size varied as the eddy center moved west. The eddy center moving speed seemed to be proportional to that of the eddy size variation. Seventy days later, the eastern half of the eddy dwindled and the whole eddy separated from the eastern boundary.

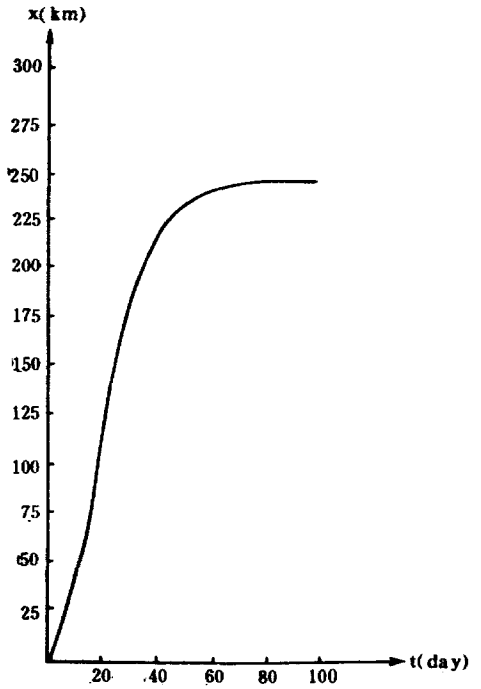

Fig. 11 Time variation of the distance between the eastern boundary and the anticyclonic eddy center

The intensity of the northeastward current grew rapidly when the anticyclonic eddy moved west. When the eddy reached the slope area both the eddy movement and the current intensification nearly stopped. By that time, the western side of the eddy had become a component of the slope current. The volume transport near the slope area was increased due to the recirculation.

Fig. 10 shows that the kinetic energy distribution is concentrated at the slope area and at the narrow strip of the western boundary. This means that the continental slope reflects most of the westward transport of the Rossby wave energy and exists as a "wall with leak". Rhines (1969) demonstrated that a step on an otherwise flat ocean floor can reflect the majority of incident Rossby waves. The intensification mechanism of the slope area indicates that the NE current here has the nature of the western boundary current and is not merely the topographical flow.

3) Influence of the eastern boundary transport

If we double the strength of the eastern boundary transport and repeat the previous numerical process, we shall find that although the structure of the flow field keeps the original form, the

locations of the characteristics shift considerably (Fig. 12). The stationary position of the eastern anticyclonic eddy was about 100 km east from that of the previous experiment. The northern wavy meander became shallower, and the western anticyclonic eddy in the shelf water shifted northeastward. By analysing the equations it can be understood that the influence of the eastern boundary condition on the interior flow is realized mainly through the nonlinear term. Numerical experiments show that the position and strength of the eddies will change with the variations of the boundary condition, the effect of the nonlinear term, and, of course, the determinant effect of the continental slope topography.

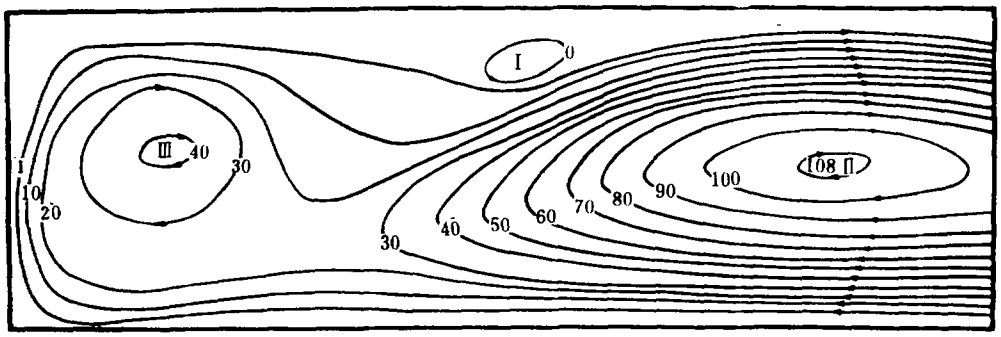

Fig. 12 Stream function contours (100* ψ) time = 60th day

9. Some conclusions

Though done under simplified conditions, our numerical experiments reveal several important factors in the nonwind-driven current forming mechanism in the northern South China Sea. The eastern incoming transport is an external forcing mechanism of the whole circulation, but the topographical restriction by the NE–SW stretching continental slope controls the major features. The continental slope can not only deflect part of the westward flow to form the slope area NE current, but also reflect most of the incident Rossby waves to intensify the NE current. The extension of the western boundary current meanders as a topography–induced Rossby stationary wave. The anticyclonic eddy detached from the eastern boundary moves westward under the β effect. Both of them also make contributions to the South China Sea Warm Current.

III. FROM THE OBSERVATION DATA

The observation data set analysed in this paper was obtained by the Japanese vessel RYOFU MARU on February 24, 1967. From Figs. 13 and 14 a warm center of high salinity could be distinguished near 20°42′N, 118°22′E. Its water mass characteristics indicated that it may have originated from the western Pacific. According to the dynamic computation, it is within an anticyclonic circulation, and its northern part is just the position of the South China Sea Warm Current. Very like the Loop Current of the Gulf of Mexico, this anticyclonic circulation seems to be formed by the extension of the Kuroshio branch (or a part pinched off from it) in the Bashi Strait.

It has been found (Huang Qizhou, 1984) that eddies are often located in the Kuroshio branch of the Bashi Strait, southwest of Taiwan and the adjacent water of Tungsha Island. In Fig. 2 an anticyclonic eddy also appears within these areas. There is a possibility that these discovered eddies had the same origin: they were separated from the Kuroshio branch, and then moved west to the

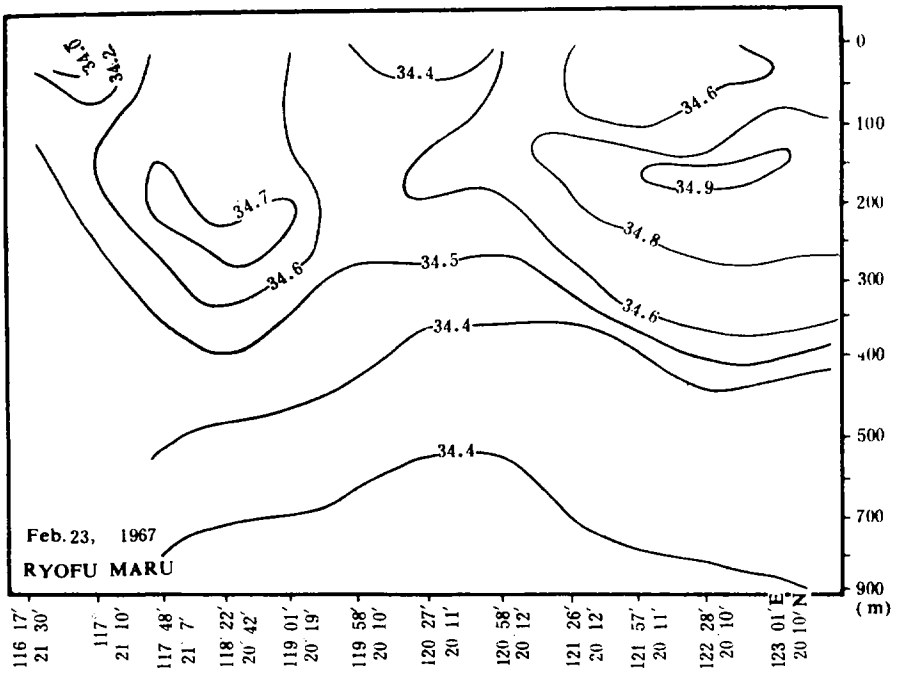

Fig. 13 Salinity section (Feb. 23 1967, in the northern South China Sea)

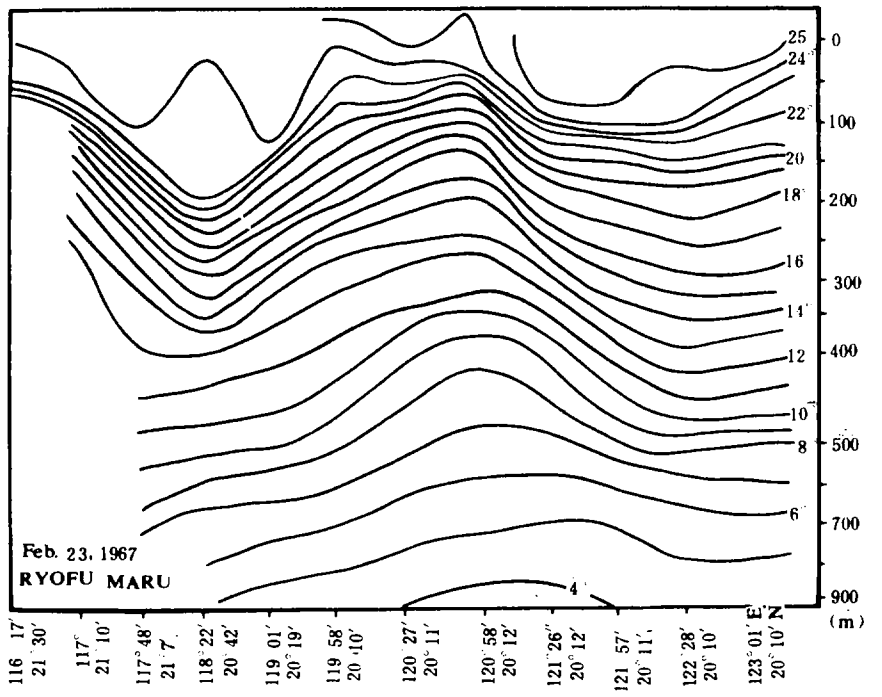

Fig. 14 Temperature section (°C) (Feb. 23, 1967, in the northern South China Sea)

various positions. This hypothesis has its theoretical basis; our numerical experiments also support it. So the β effect induced westward movement causes the mesoscale anticyclonic eddies to shift several hundred km away from their origin area, to provide energy and water volume transport to the South China Sea Warm Current. Besides, this intrusion of the high salinity water should play an important role in the replenishing process of salt in the South China Sea. These points of view should be verified in future oceanic observations.

IV. DISCUSSION

The tropical and subtropical current systems are strongly influenced by, and closely reflect, the seasonal and inter-annual variations of the prevailing winds. But for the western boundary area where the local wind effect could be neglected (except for the very thin surface layer), the total effect of the wind system upon the ocean is the overwhelming factor. This can also be explained by the western boundary transport equation: $Q_b = \int_{x_E}^{x_W} \mathrm{curl}\tau \, dx$.

Fig. 15, based on the computation data of the wind stress curl value in the North Pacific Trade Wind Zone (Guan Bingxian and Liu Jiuping, in press), shows that the negative wind stress curl value in winter is much higher than that in summer. This should cause the total southward Sverdrup transport and the North Equatorial Current to be strong in winter and relatively weak in summer. Connected with the ocean by the Bashi Strait, the northern part of the South China Sea exists as a part of the western boundary of the North Pacific. For this reason, it would inevitably be influenced by the previously described variations in the ocean interior. It seems acceptable to explain the seasonal variation of the South China Sea Warm Current in this way.

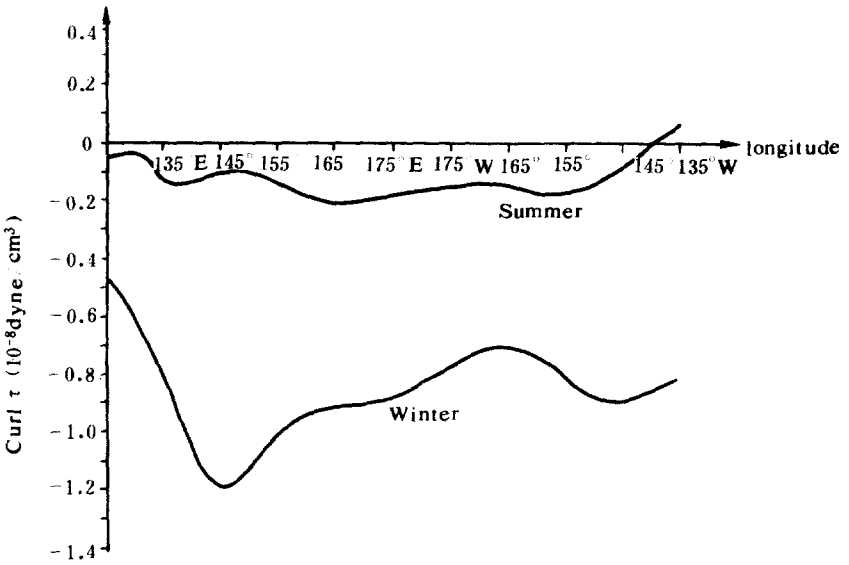

Fig. 15 Mean zonal distribution of the wind stress curl in the North Pacific Trade Wind Zone (3 year averaged value from 1968–1970)

ACKNOWLEDGMENTS

The author wishes to express her gratitude to Prof. Guan Bingxian for his guidance and

support to this work and also wishes to thank Prof. Feng Shizuo and Prof. Fang Guohong for their critical reviewing of the manuscript and valuable suggestions. The author is likewise grateful to her group colleagues for their helpful discussions and to the Shandong Computation Center for its support in the numerical work.

References

[1] Chao, S.Y., and Julian, P.C., Jr., 1982. A numerical study of the Kuroshio south of Japan. *J. Phy. Ocean.* **12**: 679—693.

[2] Endoh, M., 1973. A numerical experiment on the variations of western boundary currents, Part I. *J. Ocean. Soc. Japan* **29**: 16—27.

[3] Greenspan, H.P., 1963. A note concerning topography and inertial currents. *J. Mar. Res.* **21**(3): 147—154.

[4] Guan Bingxian, 1978. The South China Sea Warm Current-an against wind current off Guangdong Province in winter. *Ocean. Limn. Sinica* **9**(2): 117—127. (in Chinese with English abstract)

[5] Gue Zhungxien, Yang Tianhung and Chou Dezhung, 1985. The South China Sea Warm Current and its right side SW current in winter. *Tropic Ocean* **4**(1): 1—9. (in Chinese)

[6] He Chungben and Guan Bingxian, 1984. The analysis of the temperature and salinity structure of the NE-SW section in the middle South China Sea and the origin of the cold water in the basin. *Ocean. Limn. Sinica* **15**(5): 411—418. (in Chinese with English abstract)

[7] Holland, W.R., 1967. On the wind-driven circulation in an ocean with bottom topography. *Tellus* XIX: 584—600.

[8] Huang Qizhou, 1983. The velocity and transport variation of the Kuroshio in the Bashi Strait. *Tropic Ocean* **2**(1): 35—41. (in Chinese)

[9] Huang Qizhou, 1984. The oceanology state in the Bashi Strait. *Nan Hai Stu. Mar. Sinica* **6**:53—67. (in Chinese)

[10] McWilliams, J.C., and Glenn R.F., 1979. On the evolution of isolated, nonlinear vortices. *J. Phy. Ocean* **9**: 1155—1182.

[11] Pearson, C., 1965. A computational method for viscous flow problems. *J. Fluid Mech.* **21**:611—622.

[12] Rhines, P.B., 1969. Slow oscilations in an ocean of varying depth. *J. Fluid Mech.* **37**:161—189.

[13] Warren, B.A., 1967. Notes on translatory movement of rings of current with application to Gulf Stream eddies. *Deep-Sea Res.* **14**:505—524.

[14] Wyrtki, K., 1961. Physical Oceanography of the South-East Asian Waters. Scientific result of Marine Investigation of South China Sea and Gulf of Thailand 1959—1961, Naga Report 2, pp. 2—195.